

Vehicle Black Box with 24GHz FMCW Radar

Jung-Hwan Kim, Sun-Kyu Kim, Sang-Hyuk Lee, Tae-Min Lee and Joonhong Lim

Department of Electronic Systems Engineering, Hanyang University

Seoul, Republic of Korea

{ angelkim88, jhlim } @hanyang.ac.kr

Abstract— This paper presents vehicle black box using camera image and 24GHz Frequency Modulation Continuous Wave (FMCW) radar. Currently, almost all of vehicle black boxes are recording driving data using a single camera. They have some problems on low image quality and narrow viewing angle. In addition, it is difficult to record a clean image when the weather is in bad condition due to heavy rain, snow and night. These problems may have some troubles to investigate car accident accurately. In this paper, we propose a novel black box fusing data from radar and cameras. We estimate the distance and velocity of obstacle using the Doppler Effect and FMCW radar. In particular, we compare various Direction of Arrival (DOA) algorithms for estimation of obstacle angle. The experimental results indicate that the Multiple Signal Classification (MUSIC) is more accurate compared to other methods. Moreover, we formulate the vehicle tracking image through the camera image processing and radar information. This image can be used to widen viewing angle and it may be helpful to investigate a car accident. The experimental study results indicate that the new black box overcome the disadvantages of the current black boxes and may be useful for safe driving and accurate accident investigation.

Keywords—FMCW Radar; Vehicle Black Box; Camera Image Processing; Beamforming; DOA; MUSIC; Root-MUSIC;

I. INTRODUCTION

Recently, high end automobiles have forward collision warning system as there are many researches about Advanced Driver Assistance Systems (ADAS). On the other hand, there are relatively a little research about systems for automobile accident investigation. Automobile accident investigation methods have not changed for a long time since vehicle was developed. Investigator is still collecting evidence using old methods such as measurements of the skid mark, statements of witness and scene photographs. These methods have low reliability of the results of an investigation. To overcome this shortfall, some insurance companies encourage drivers to install black box in their cars. Recorded data in black box help an investigator to investigate an accurate cause of accident. However, the recorded data have some problems on such as low quality image and narrow view, because almost all of vehicle black boxes are recording driving data using only a single camera. In addition, the current black boxes are affected by a surrounding environments such as temperature, humidity and bad weather[1].

In this paper, In order to overcome these disadvantages, we propose the new black box fusing 24GHz FMCW radar and camera image processing. We measure distance and velocity of front obstacle/vehicle using the Doppler Effect. Moreover,

angle of front obstacle is estimated using DOA algorithms and Uniform Linear Array (ULA) antenna[2-4]. Vehicle tracking image is created using digital image processing[5]. Fig. 1 shows the proposed systems using radar and camera.

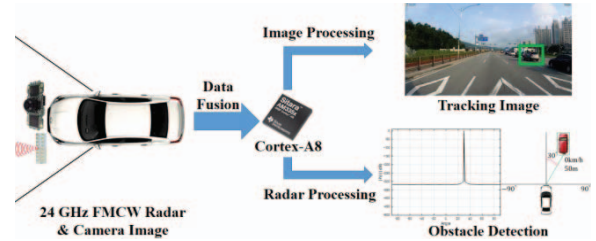


Fig. 1. The proposed black box systems using radar and camera.

II. 24 GHz FMCW RADAR

A. Operation Principle of FMCW Radar

A conventional pulse radar measure the distance using the single signal, so this radar has delay time until the system received the returned transmission signal from the reflecting object. On the other hand, FMCW radar does not have time delay while distance and velocity are measured since this radar uses continuous wave radar system. The advantages of FMCW are more high resolution and low power than the conventional pulse radar. Therefore, FMCW radar is widely used for automobile radar systems.

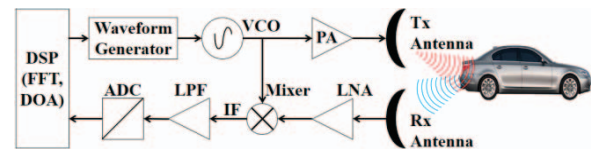


Fig. 2. 24GHz FMCW Radar Block Diagram.

As shown in Fig. 2, The modulated frequency signal is created through the waveform generator and Voltage Controlled Oscillator (VCO). This modulated signal is amplified using power amplification (PA), and the amplified signal is transmitted through the TX antenna. The received signal through the RX antenna is a weak signal containing noise. The Low Noise Amplification (LNA) can be used eliminate noise and make strong signal. The Intermediate Frequency (IF) signal is created that the transmitted and received signal are mixed by the mixer. A noise in the IF signal is removed using the Low Pass Filter (LPF), then we can know a beat frequency by this IF. A digital beat frequency is created

This research was supported by Ansan-Si hidden champion fostering and supporting funded by Ansan city.

by the Analog to Digital Converter (ADC). Finally, distance and velocity of object can be determined using the Fast Fourier Transform (FFT) and Doppler Effect.

B. Distance and Velocity Measurement

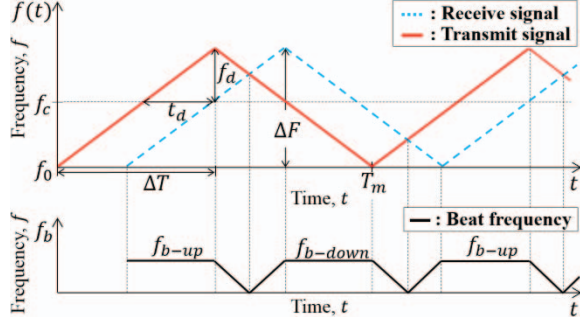


Fig. 3. The relation between FMCW Signal and Beat Frequency.

As shown in Fig. 3, the shape of modulated frequency is triangular waveform. This waveform can be divided into two parts that are increasing and decreasing interval. The increasing interval frequency $f_{t-up}(t)$ can be written as

$$f_{t-up}(t) = f_0 + \alpha t, \quad 0 < t < \Delta T. \quad (1)$$

The decreasing interval frequency $f_{t-down}(t)$ is

$$f_{t-down}(t) = f_0 + \alpha t, \quad \Delta T < t < T_m. \quad (2)$$

here, T_m is the modulation period and f_0 is start frequency. The change rate α of frequency per time is defined as

$$\alpha = \frac{df}{dt} = \frac{\Delta F}{\Delta T} \quad (3)$$

where ΔF is the frequency excursion, and the half of modulation period is denoted as ΔT . In a frequency phase that is zero at time $t = 0$, the transmitted signal of increasing and decreasing interval can be given as follows:

$$S_{t-up}(t) = a \cdot \cos 2\pi \int_0^t f_{t-up}(t) dx, \quad (4)$$

$$S_{t-down}(t) = a \cdot \cos 2\pi \int_0^t f_{t-down}(t) dx. \quad (5)$$

On the other hand, The received signal of increasing and decreasing interval can be expressed as

$$S_{r-up}(t) = \frac{b}{a} S_{t-up}(t - t_d), \quad (6)$$

$$S_{r-down}(t) = \frac{b}{a} S_{t-down}(t - t_d) \quad (7)$$

by the delay time t_d and the Doppler frequency shift f_d which is a difference between transmitted and received frequency. The parameter b is an attenuation of radio wave by round trip distance. As shown in Fig. 2, The IF signal filtered by the LPF is the beat frequency. During the increasing interval, $t_d < t < \Delta T$, beat frequency $S_{b-up}(t)$ can be written as

$$S_{b-up}(t) = c \cdot \cos 2\pi [f_0 t_d + f_d(t - t_d) - \frac{\alpha}{2} t_d^2 + \alpha t_d t] \quad (8)$$

Meanwhile during the decreasing interval, $\Delta T + t_d < t < 2\Delta$

$+t_d$, beat frequency $S_{b-down}(t)$ is given as

$$S_{b-down}(t) = c \cdot \cos 2\pi [(f_0 + \Delta F)t_d + f_d(t - t_d) + \frac{\alpha}{2} t_d^2 - \alpha t_d t] \quad (9)$$

where c is the conversion loss of mixer. Finally, the frequency content αt_d of beat frequency signal $S_b(t)$ becomes the beat frequency f_b , that is

$$\alpha t_d = f_b = \frac{\Delta F \cdot 2R}{\Delta T \cdot \tau} \quad (10)$$

where τ is velocity of radio wave and R is the distance of object. When an object does not move, the Doppler frequency shift f_d is zero as in Fig. 3. Therefore, the beat frequency f_b becomes a range frequency f_r . The distance R to the reflecting object can be obtained using the range frequency f_r and Eq. (10). This leads to

$$R = \frac{\tau \cdot t_d}{2} = \frac{\Delta T \cdot \tau \cdot f_r}{2 \cdot \Delta F}. \quad (11)$$

If the object is moving, a Doppler frequency shift f_d will be superimposed to the beat frequency f_b . The relations of Doppler and beat frequency are tabulated in table 1 as follows:

TABLE I. RELATION OF DOPPLER AND BEAT FREQUENCY

	Moving direction of object	f_{b-up}	f_{b-down}
$f_r > f_d$	Object moving toward the radar	$f_r - f_d$	$f_r + f_d$
	Object moving away from the radar	$f_r + f_d$	$f_r - f_d$
$f_r < f_d$	Object moving toward the radar	$f_d - f_r$	$f_d + f_r$
	Object moving away from the radar	$f_d + f_r$	$f_d - f_r$

In the case that range frequency is greater than Doppler frequency, The range frequency can be obtained from the beat frequency of increasing and decreasing interval as

$$f_r = \frac{f_{b-up} + f_{b-down}}{2}. \quad (12)$$

Doppler frequency also can be extracted as

$$f_d = \frac{f_{b-down} - f_{b-up}}{2}. \quad (13)$$

At this time, the velocity V_r of object is measured by

$$V_r = \frac{c \cdot f_d}{2 \cdot f_0}. \quad (14)$$

III. DOA ESTIMATION ALGORITHMS

A. The modeling of incident signal

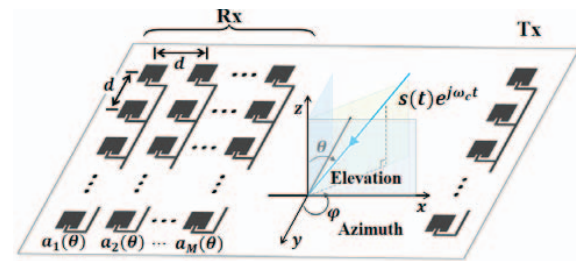


Fig. 4. DOA estimation with microstrip patch antenna array.

As shown in Fig. 4, Arriving complex sinusoidal signal $\hat{x}_M(t)$

in M th antenna can be modeled from

$$\hat{x}_M(t) = s(t)e^{j\omega_c\left(t - \frac{r_M^T u}{c}\right)} = a_M(\theta)s(t)e^{j\omega_c t}. \quad (15)$$

The expression is based on the narrowband signal assumption that the approximation $s(t - \tau_M) \cong s(t)$ holds[6]. Here, u is the direction cosine of incident signal, c is the propagation velocity of signal, and r_M is the position vector of antenna. $s(t)$ is the signal source which has an information, θ is the elevation angle of incident signal, and ω_c is the center frequency of signal. Eq.(15) can be expressed as a vector given by

$$X(t) = \begin{bmatrix} x_1(t) \\ x_2(t) \\ \vdots \\ x_M(t) \end{bmatrix} = \begin{bmatrix} a_1(\theta) \\ a_2(\theta) \\ \vdots \\ a_M(\theta) \end{bmatrix} s(t) = a(\theta)s(t), \quad (16)$$

where $a(\theta)$ is called array steering vector. For multiple signal and white Gaussian additive noise $n_M(t)$, the equation can be written as

$$X(t) = A(\theta)S(t) + N(t), \quad (17)$$

where $A(\theta)$ is called array manifold matrix which has direction information of incident signal. As shown in Fig. 4, Steering vector of ULA can be written as

$$a_{ULA}(\theta) = [1 \quad e^{-jQd\cos\theta} \quad \dots \quad e^{-j(M-1)Qd\cos\theta}]^T, \quad (18)$$

$$k = \frac{\omega_c}{c} = \frac{2\pi}{\lambda}. \quad (19)$$

where d is the Inter-element spacing of a linear equispaced array and λ is the wavelength of signal.

B. DOA Estimation using spectral methods

As shown in Fig. 5, the classical beamformer structure has an output signal $y(t)$ and is given by a linearly weighted sum of the sensor element[9-11].

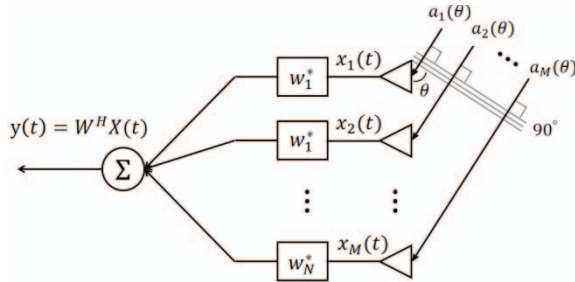


Fig. 5. Typical M-element uniform linear array with arriving signals.

Spectral methods estimate DOA using the spatial spectrum, that is, the mean power received by an array as a function of θ , and then determining the local maxima of this computed spatial spectrum[7]. The output power spectrum of array is given by

$$p(W) = \frac{1}{N} \sum_{t=1}^N |y(t)|^2 = W^H \hat{R} W \quad (20)$$

where superscript H denotes complex conjugate transpose of a matrix. Depending on the method of determining weight vector

W , various beamforming algorithms are define as follows: In general, weight vector W is given by the steering vector $a(\theta)$ and function of spatial correlation matrix R .

1) *Conventional Beamforming (CB)* : CB algorithm is the spectrum analysis using a Fourier transform in space which gives the weight to the incident signal for increasing signal to noise ratio (SNR) and maximum output[2-4, 8]. The CB weight vector W_{CB} which is the solution for

$$\max_W E[W^H X(t)X^H(t)W]. \quad (21)$$

can be expressed as

$$W_{CB} = \frac{a(\theta)}{\sqrt{a^H(\theta)a(\theta)}}. \quad (22)$$

The conventional beamforming space spectrum can be obtained from the power spectrum and weight vector as

$$P_{CB}(\theta) = \frac{a^H(\theta)\hat{R}a(\theta)}{a^H(\theta)a(\theta)}. \quad (23)$$

2) *Maximum Likelihood (ML) Method* : The ML method is a minimum variance distortionless response beamformer, which finds the ML estimate of the power arriving from a point source in direction assuming all other sources as interferences. The ML weight vector W_{ML} which is the solution for

$$\min_W W^H \hat{R} W \quad \text{subject to } W^H a(\theta) = 1, \quad (24)$$

is given by

$$W_{ML} = \frac{\hat{R}^{-1}a(\theta)}{a^H(\theta)\hat{R}^{-1}a(\theta)}. \quad (25)$$

Replacing the weight vector W_{ML} in Eq.(20) yields to the ML beamforming space spectrum which is

$$P_{ML}(\theta) = \frac{1}{a^H(\theta)\hat{R}^{-1}a(\theta)}. \quad (26)$$

3) *MUSIC method* : This method is based on spectral estimation which exploits the orthogonality of the noise subspace with the signal subspace[8]. The eigenvalue decomposition of array correlation matrix R is

$$R = ASA^H + \sigma_n^2 I = U_s \Lambda_s U_s^H + \sigma_n^2 U_n U_n^H. \quad (27)$$

The signal subspace U_s is orthogonal to the noise subspace U_n which means that

$$\text{span}(R_s) = \text{span}(A) = \text{span}(U_s). \quad (28)$$

$$U_n^H a(\theta) = a^H(\theta)U_n U_n^H a(\theta) = 0. \quad (29)$$

The MUSIC pseudospectrum can be written as

$$P_{MUSIC}(\theta) = \frac{1}{a^H(\theta)U_n U_n^H a(\theta)}. \quad (30)$$

4) *Root-MUSIC method* : This method is the modification of the MUSIC algorithm that have been proposed to increase the resolution and reduce the computational complexity[2-4,12]. Root-MUSIC is based on polynomial rooting. So this

method is called Root-MUSIC. The denominator in Eq.(30) can be written as

$$a^H(\theta)Ca(\theta) = \sum_{l=1}^{M-1} c_l e^{jkd l \sin \theta}. \quad (31)$$

where the matrix C is $U_n U_n^H$ and c_l is the sum of the diagonal elements of C along the l -th diagonal. Eq.(31) can be simplified to be in the form of a polynomial given by

$$D(z) = \sum_{l=1}^{M-1} c_l z^l. \quad (32)$$

where z is $e^{-jkd \sin \theta}$. The roots of $D(z)$ closest to the unit circle correspond to the poles of Eq.(30). That is why Exact zeroes in $D(z)$ exist when $|z_i| = 1$. The DOA can be obtained by comparing $e^{j \arg(z_i)}$ to $e^{jkd \sin \theta_i}$ to get

$$\sin \theta_i = -\frac{1}{kd} \arg(z_i), \quad (33)$$

where $\arg(z_i)$ is the phase angle of z_i [11-13].

IV. SIMULATION RESULTS

In this paper, the DOA, velocity and distance of object are simulated using a MATLAB. Table 2 shows radar parameter.

TABLE II. PARAMETER VALUES OF 24GHz FMCW RADAR

Parameters	Symbol	Value	Unit
Center frequency	f_c	24	GHz
Frequency excursion	ΔF	200	MHz
Sampling frequency	f_s	2.52	MHz
Sweep Time	ΔT	10	ms
FFT point	N_{FFT}	10000	-
Antenna elements (ULA)	M	6	-
Antenna inter-element spacing	d	0.5	-

We assume Gaussian distributed noise of variance σ_n^2 is 0.1, and the object which is in front of the vehicle is located at the distance of 50m. The velocity of this object is 80km/h. In the case of Fig. 6 where object is coming toward the radar, velocity and distance of the object can be obtained by Eq.(11) and Eq.(14). The simulation results of velocity and distance using the beat frequency FFT in Fig.6 are 51.85m and 77.85km/h. The error rates of distance and velocity are approximately 3% and 6%.

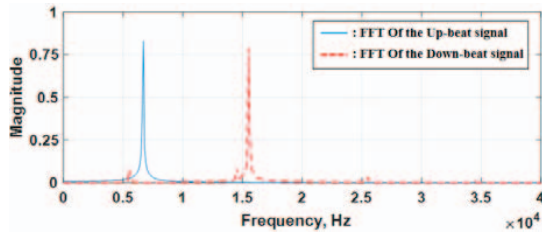


Fig. 6. The FFT of beat frequency at up and down chirp.

The methods of CB, ML and MUSIC are used with the six element array antenna for the DOA estimation. On the other hand, Root-MUSIC method is used with four element array

antenna. Fig 7. shows that the estimated DOA results of two objects, which are located at the angle of -20° and 0° .

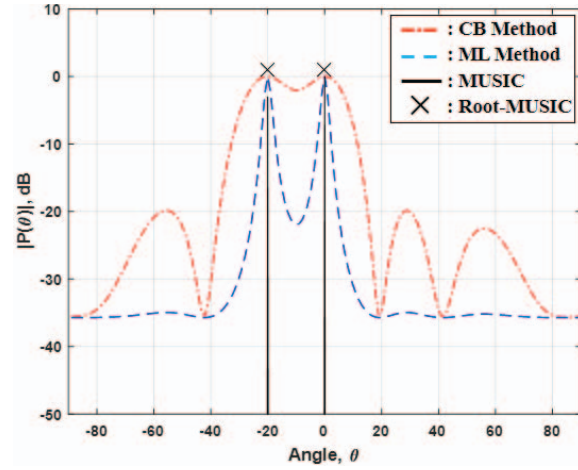


Fig. 7. The simulation results of Estimated DOA using MATLAB.

The root-MUSIC polynomial coefficients are given by the sums along the $2(M-1) = 6$ diagonals as follows:

$$c = -.009 - .271i, -.070 + .128i, -.921 + .545i, 2, \\ -.921 - .545i, -.070 - .128i, -.009 + .271i \quad (34)$$

We can find the roots and then solve for the magnitude and angles using root command in MATLAB. The matrix R of roots by Eq.(34) can find

$$R = \begin{bmatrix} -2.1247 - 1.2421i \\ -0.3508 - 0.2051i \\ 0.4868 + 0.8930i \\ 0.4706 + 0.8633i \\ 1.0117 - 0.0108i \\ 0.9884 - 0.0106i \end{bmatrix}. \quad (35)$$

All 6 roots are plotted in Fig. 8 where the distance to the unit circles can be shown. It is clear that only the four on the right side of the y-axis are nearest to the unit circle and are close to the expected angles of arrival. The other two roots are excluded

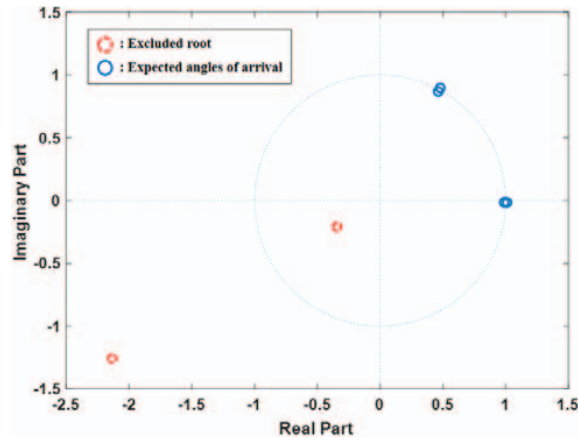


Fig. 8. All 6 roots in cartesian coordinates of Root-MUSIC.

because they are not near the unit circle.

Table 3 shows processing speed of each DOA algorithms with six antennas. The measured values are averages which were performed 20 times. Processing time was measured using tic, toc function in MATLAB. Processor specifications of computer are Intel(R) Core(TM) i7-4790 and 8GB RAM. CPU clock is 3.6 GHz. Processing time of the Root-MUSIC is approximately five times faster than the MUSIC.

TABLE III. ALGORITHMS PROCESSING TIME

Algorithms	Antenna	Processing Time	Unit
Conventional Beamforming	6	0.196784	Sec
Maximum Likelihood	6	0.179555	Sec
MUSIC	6	0.158473	Sec
Root-MUSIC	6	0.029049	Sec

We integrate the Root-MUSIC algorithm and black box image. Fig. 9 shows that the simulation results of proposed vehicle black box system using MATLAB. Fig 9 (a) is image that assume the two objects which are located at the distance of 50m in front of the vehicle in the daytime. Fig. 9 (b) is the final result image in the night.



Fig. 9. The simulation results of proposed vehicle black box system using MATLAB. (a) Image processing of tracking two object in the daytime. (b) Image processing of tracking two object in the night.

V. CONCLUSION

Most existing devices for vehicle black box have problems with narrow view and low quality image by a surrounding environment. To overcome this shortfall, we propose a new black box with 24GHz FMCW radar in this paper. As shown in

Fig. 7 and Table. 3, the simulation results validate that the Root-MUSIC method has a better performance than other methods. The CB is not suitable in the narrow space like vehicle, because the resolution is determined by the number of sensors. The disadvantage of ML method is that resolution is affected by the small size of array aperture and the low SNR. The processing speed of MUSIC is approximately five times slower than Root-MUSIC. Therefore, Root-MUSIC is more suitable for the vehicle radar. If Root-MUSIC method and camera image processing are utilized for the proposed black box, it will be helpful for viewing angle expansion and accurate accident investigation. In addition, it is possible to prevent a car accident since it will help to detect object in a bad environment as shown in Fig. 9 (b).

The future study may include developing the smart black box with the four channel cameras, OBD and DOA algorithms. Also we will investigate methods to construct panorama images using the four channel cameras in order to eliminate blind spot.

REFERENCES

- [1] Christian Simon, "Reflection removal for in-vehicle black box videos", IEEE Conf. Computer Vision and Pattern Recognition, pp. 4231-4239, June 2015.
- [2] Merrill I. Skolnik, Introduction to RADAR systems. Third edition, Columbus, CA: McGraw-Hill, 2002.
- [3] Bassem R. Mahafza, Radar Systems Analysis and Design Using MATLAB. Second edition, London, CA: Chapamn & Hall/CRC, 2005.
- [4] Bassem R. Mahafza, Radar systems analysis and design using Matlab. London, CA: Chapamn & Hall/CRC, 2000.
- [5] Rafael C. Gonzalez, Digital Image Processing using MATLAB. London, CA: Pearson, 2004.
- [6] Moon-Sik Lee, "Signal Modeling and Analysis of a Planar Phased-Array FMCW Radar with Antenna Switching", IEEE Antennas and Wireless Propagation Letters, vol. 10, pp. 179-182, March 2011.
- [7] Zhang, Q.T, "A statistical resolution theory of the beamformer-based spatial spectrum for determining the directions of signals in white noise", IEEE Transactions on Signal Processing, vol. 43, issue 8, pp. 1867-1873, August 1995.
- [8] Peter Wenig, Michael Schoor, Oliver Gunther, Bin Yang, "System Design of a 77 GHz Automotive Radar Sensor with Superresolution DOA Estimation", IEEE International Symposium on Signals, Systems and Electronics, pp. 537-540, August 2007.
- [9] B. Allen, M. Ghavami, Asaptive array systems fundamentals and applications. First edition, England, CA: Wiley, 2005.
- [10] Sathish Chandran, Advances in direction of arrival estimation. First edition, Norwood, CA: Artech house, 2006.
- [11] Harry L. Van Trees, Optimum array processing : Part IV of detection, estimation, and modulation theory. First edition, England, CA: Wiley, 2002.
- [12] De Leon, F.A. Marciano, J.J.S., "Application of MUSIC, ESPRIT and SAGE Algorithms for Narrowband Signal Detection and Localization", TENCON IEEE Region 10 Conference, pp. 1-4, November 2006
- [13] Yanping Liao, Aya Abouzaid, "Resolution Improvement for MUSIC and ROOT MUSIC Algorithms", Journal of Information Hiding and Multimedia Signal Processing Ubiquitous International, pp. 189-197, march 2015